How to cite: *Angew. Chem. Int. Ed.* **2020**, *59*, 14992–14999
International Edition: doi.org/10.1002/anie.202005372
German Edition: doi.org/10.1002/ange.202005372

Predictive Models

A Predictive Model Towards Site-Selective Metalations of Functionalized Heterocycles, Arenes, Olefins, and Alkanes using TMPZnCl·LiCl

*Moritz Balkenhohl[+], Harish Jangra[+], Ilya S. Makarov, Shu-Mei Yang, Hendrik Zipse, and Paul Knochel**

In memory of Professor Rolf Huisgen

Abstract: *The development of a predictive model towards site-selective deprotometalation reactions using TMPZnCl·LiCl is reported (TMP = 2,2,6,6-tetramethylpiperidinyl). The pK_a values of functionalized N-, S-, and O-heterocycles, arenes, alkenes, or alkanes were calculated and compared to the experimental deprotonation sites. Large overlap (>80%) between the calculated and empirical deprotonation sites was observed, showing that thermodynamic factors strongly govern the metalation regioselectivity. In the case of olefins, calculated frozen state energies of the deprotonated substrates allowed a more accurate prediction. Additionally, various new N-heterocycles were analyzed and the metalation regioselectivities rationalized using the predictive model.*

Introduction

Polyfunctional arenes and heteroarenes are important classes of small molecules, as they find major applications as building blocks in pharmaceutical and agrochemical research today.[1] Almost every newly approved small molecule drug by the United States Food and Drug Administration (FDA) in 2018 contains a (hetero)arene moiety, demonstrating their utmost importance in modern pharmaceutical research.[2] Therefore, the regioselective functionalization of various (hetero)aryl scaffolds is of highest interest and has been addressed by numerous research groups in the past decades.[3]

A straightforward method to selectively introduce a functional group to a (hetero)arene core is its directed metalation, followed by electrophilic trapping reactions.[4] Recently, deprotometalations of arenes and heteroarenes using metal amide bases have allowed the regioselective introduction of a broad range of functional groups to a plethora of important substrates.[4] Both highly reactive lithium amides, such as LDA[5] or TMPLi[6] (TMP = 2,2,6,6-tetramethylpiperidinyl), or more selective reagents such as TMPMgCl·LiCl[7] or TMPZnCl·LiCl[8] have been used successfully. This gave access to functionalized arenes or heteroarenes, including pharmaceutically relevant scaffolds such as pyrimidines, pyrazines or pyridazines.[8c,9] However, when novel scaffolds were investigated towards directed metalation reactions, the regioselectivity was difficult to anticipate and had to be determined by experimental methods.[7,8] This tedious and inefficient approach hampers a rapid and straightforward systematic functionalization of new heterocycles of the future.

So far, pK_a calculations have been used to understand experimental results in deprotometalation reactions using magnesium or lithium amides.[8c,10] With these theoretical studies, regioselectivities could indeed be explained, whereas a reliable prediction has not yet been possible. The difficulty to selectively predict the deprotonation site in a molecule arises from several competing kinetic and thermodynamic effects which must be considered in the deprotonation process.[10] Thus, thermodynamic considerations mainly focus on the acidity of the proton and the concomitant stability of the resulting anion for determining the deprotonation site. This stability can be influenced by electron donating or electron withdrawing groups, which may destabilize or stabilize the resulting negative charge.[10b] However, kinetic considerations mostly favor a deprotonation adjacent to a coordination site. The base coordinates through its counterion to a Lewis basic direct metalation group (DMG) in the molecule, forming a substrate–base adduct. This brings the base in proximity to a C–H bond, which is subsequently deprotonated (complex induced proximity effect = CIPE).[11] Thus, for many bases both kinetic and thermodynamic effects play a role for determining the metalation site.

Considering, that the nitrogen–metal bond in the milder, and functional group tolerant base TMPZnCl·LiCl[8] is of more covalent nature in comparison to the magnesium and lithium analogues due to a smaller difference in electronegativity (ΔEN(N–Zn, Pauling) = 1.39, ΔEN(N–Mg) = 1.73, ΔEN(N–Li) = 2.06),[12] TMPZnCl·LiCl is a base where thermodynamic effects should predominate and the kinetic aspects should play a minor role. In fact, the stronger ionic

[*] Dr. M. Balkenhohl,[+] Dr. H. Jangra,[+] Dr. I. S. Makarov, Prof. Dr. H. Zipse, Prof. Dr. P. Knochel
Department of Chemistry, Ludwig-Maximilians-Universität München
Butenandtstr. 5–13, 81377 Munich (Germany)
E-mail: paul.knochel@cup.uni-muenchen.de
S.-M. Yang
Department of Chemistry, National (Taiwan) Normal University
88, Sec. 4, Tingchow Road, Taipei 11677 (Taiwan, Republic of China)
[+] These authors contributed equally to this work.
Supporting information and the ORCID identification number(s) for the author(s) of this article can be found under: https://doi.org/10.1002/anie.202005372.

character of the N–Met bond (Met = metal), the more likely is the kinetic control. Therefore, lithium amides are prone to metalate organic substrates under kinetic control.[5b,10,13] Thus, we envisioned, that the site selectivity of the base TMPZnCl·LiCl may go hand in hand with the lowest (calculated) pK_a values of various arenes or heteroarenes. This would allow the development of a theoretical model[14] using simple pK_a calculations, bringing forth reliable predictions for site selective deprotometalations with the mild base TMPZnCl·LiCl. Herein, we wish to report the development of such a predictive model, which not only rationalizes deprotometalations using TMPZnCl·LiCl from the past, but also allows the prediction of the metalation sites on novel, so far unexplored *N*-heterocycles.

Computational Details

Two different modelling approaches were explored to predict the preferred metalation site of the structurally diverse heterocycles as shown below. In *Approach 1*, relative C–H pK_a values are calculated for substrates R–H through the proton transfer reaction shown as Equation (1) in Scheme 1 with the furan/furan-2-ide reference system, whose pK_a value amounts to 35.0 in DMSO.[13] The conformational space of each molecular species is first explored using molecular mechanics (MM) methodology, followed by full geometry optimization with quantum chemical methods in order to obtained Boltzmann-averaged Gibbs free energies over the selected conformational space (see the Supporting Information for more details). All pK_a values shown in Figures 1–4 and 6, 7 were obtained this way.

A second strategy termed *Approach 2* was explored for those substrates, where deprotonation leads to structural rearrangement or fragmentation. For these systems vertical deprotonation energies (VDEs) in terms of ΔE_{tot} were calculated based on the substrate conformer of lowest Gibbs free energy. Deprotonation energies are calculated for the various sites relative to the furan/furan-2-ide reference system, where all anions are kept in a frozen (unrelaxed) state. The VDE values obtained this way are shown in Figure 5 for all alkene substrates and are listed in the Supporting Information for all other systems studied herein.

Computational Methodology: As in earlier studies[8c] all geometry optimizations have been performed at the B3LYP[15]-D3[16]/6-31++G(2d,p)[17] level of theory in the gas phase. Thermochemical corrections have been calculated at the same level of theory using the rigid rotor/harmonic oscillator model. Implicit solvation energies for DMSO were calculated for gas phase optimized geometries at the CPCM[18](DMSO)/B3LYP-D3/6-31++G(2d,p) level of theory, and subsequently added to gas phase single point energies obtained at the B3LYP-D3/6–311++G(2df,2p)//B3LYP-D3/6-31++G(2d,p) level of theory in order to obtain solution phase energies (see the Supporting Information for more details).

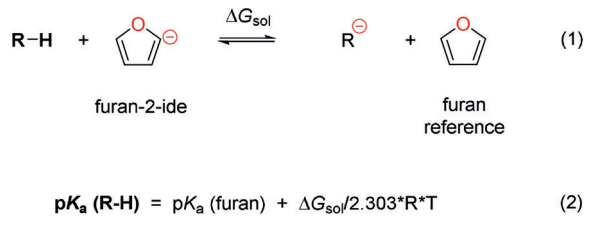

Scheme 1. Proton transfer reaction used for the pK_a calculation in solution.

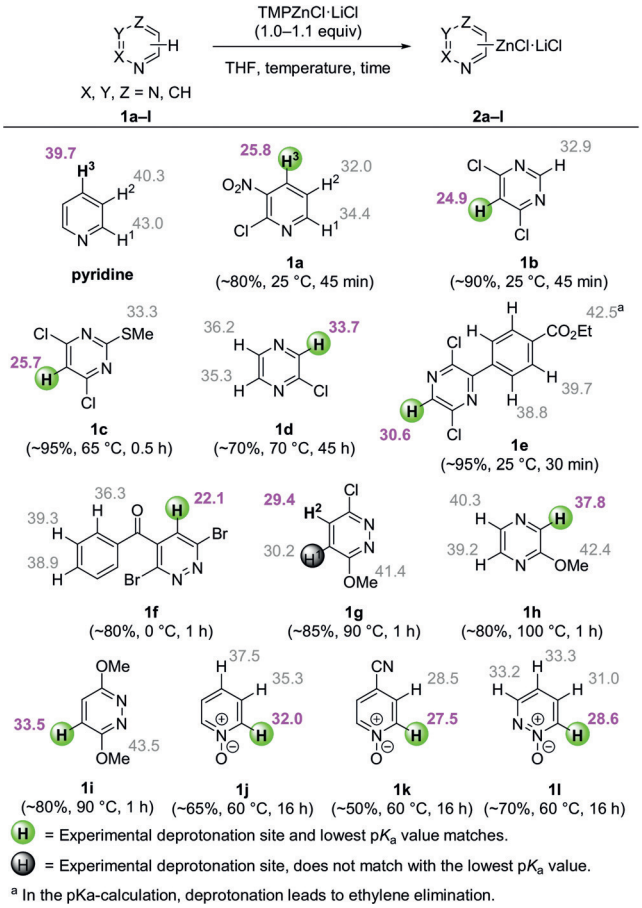

Figure 1. Calculated pK_a values of various azines, including pyridines, pyrimidines, pyrazines, and pyridazines.

Results and Discussion

As mentioned above, we anticipated that for the mild base TMPZnCl·LiCl, kinetic effects are less prone to play a role in the choice of the deprotonation site, whereas a higher importance of thermodynamic effects are expected. Thus, all substrates which have been deprotonated using TMPZnCl·LiCl were investigated and the calculated pK_a values are listed below. For each substrate class, a representative set of structures was chosen (for full experimental and theoretical details see the Supporting Information). In the following Figures 1–7 the lowest calculated pK_a value is given in purple color. When the experimental deprotonation site matches the lowest pK_a value, the proton was marked green. In the case of a mismatch (the deprotonation site did not

match with the site of lowest pK_a value) the proton was marked black. Also, the reaction conditions and yields for the resulting zinc organometallics after treatment with TMPZnCl·LiCl are given.[19]

Azines: First, we focused on a representative set of azines, including pyridines, pyrimidines, pyrazines, and pyridazines bearing various functional groups (12 out of 27 structures are depicted, Figure 1).[20] The most acidic proton of pyridine was located at the C4 position (pK_a(H3) = 39.7), followed by the proton in the C3 position (pK_a(H2) = 40.3).[21] The pK_a value at C2 was distinctly higher (pK_a(H1) = 43.0), which was explained by the neighboring *N*-atom, since the lone pair destabilizes the anion which formed upon deprotonation.[10b] When electron-withdrawing groups, such as a halogen or a nitro group, are introduced to the pyridine core, the calculated pK_a values of adjacent protons significantly decreased. This is the case for 2-chloro-3-nitropyridine (**1a**), where the pK_a value at C4 was lowest (pK_a(H3) = 25.8), which is also where deprotonation took place when **1a** was treated with TMPZnCl·LiCl (25 °C, 45 min), yielding the zinc organometallic **2a** in about 80 % yield (Figure 1).[22] Similarly as in **1a**, halogen substituents also decreased the pK_a value of *ortho*-positioned protons significantly (**1b–g**). Thus, the pK_a values in pyrimidines **1b**,**c**,[22,23] pyrazines **1d**,**e**,[24,9e] or pyridazine **1f**[9f] were lowest *ortho* to the halogen atom, which corresponded to the actual deprotonation sites, producing organozinc reagents **2b–f** in 70–95 % yield (25–90 °C, 0.5–1 h). However, in the case of pyridazine **1g**,[23] the previously described complex induced proximity effect (CIPE) predominated the thermodynamically favored position, which resulted in a deprotonation *ortho* to the directing methoxy group (pK_a(H1) = 30.2, 90 °C, 1 h) rather than the site of lowest pK_a value (pK_a(H2) = 29.4). When solely methoxy groups were present (**1h**,**i**) the protons with the lowest pK_a values (pK_a = 33.5–37.8) were deprotonated by the zinc amide base under harsher reaction conditions (ca. 80 %, 90–100 °C, 1 h).[23] Additionally, the pK_a values of pyridine and pyridazine *N*-oxides were calculated and compared with the experimental deprotonation sites. The N–O bond removes electron density from the heterocycle, acidifying the protons in the aromatic ring. Thus, protons *ortho* to the *N*-oxide were acidified most (**1j–l**), which again matches the experimentally determined deprotonation sites, leading to the corresponding zinc reagents **2j–l** in 50–70 % yield (Figure 1).[25]

Other N-Heterocycles: Next, other nitrogen containing heterocycles were investigated (12 out of 30 structures are depicted in Figure 2).[20] A protected indole bearing an aldehyde functional group **3a** was deprotonated in the predicted position (pK_a(H1) = 29.5, 25 °C, 0.5 h), which led to the desired organozinc **4a** in about 90 % yield.[23] Other indole derivatives, such as pyrazolo[1,5-*a*]pyridine (**3b**),[26] or indazole **3c**[27] were also predicted correctly (pK_a(H1) = 31.1–32.4), producing zinc organometallics **4b**,**c** in 80–90 % yield. Also, the pK_a values of various purine derivatives (**3d–f**) were analyzed, where deprotonation took place in the predicted C8 position within a small pK_a range of pK_a(H1) = 28.2–29.5. Thus, after deprotonation using TMPZnCl·LiCl (25 °C, 5–30 min), the desired purine zinc species **4d–f** were obtained in 75–85 % yield.[22,28] When a 1,2,4-triazole bearing an amide

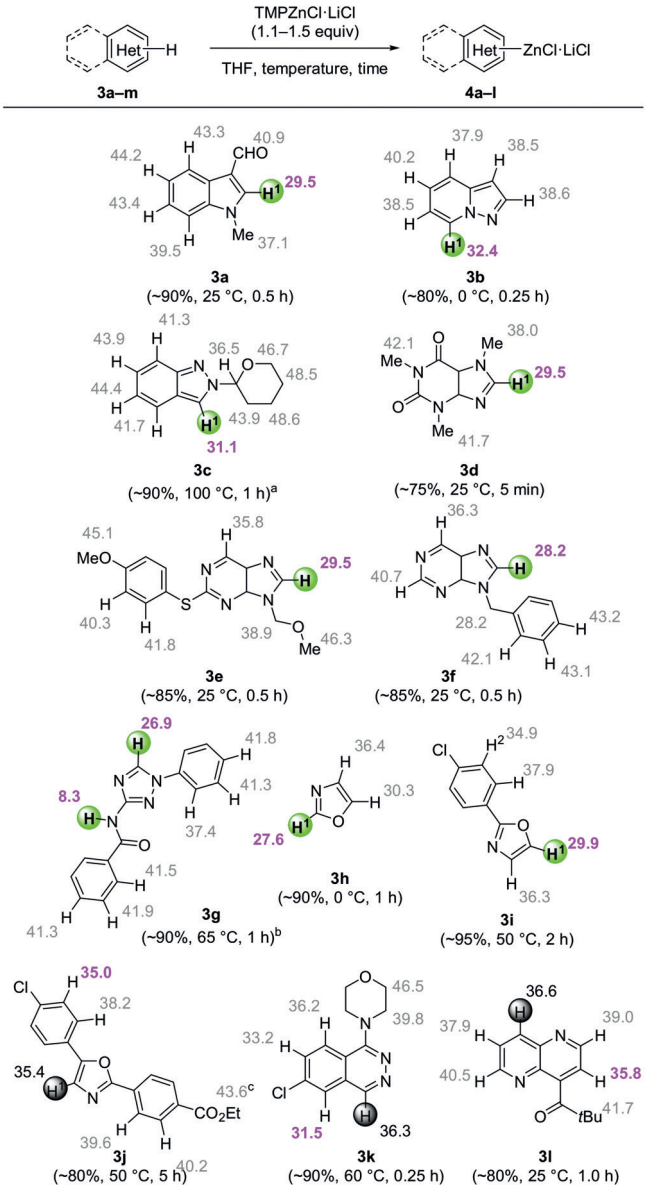

Figure 2. Calculated pK_a values of other *N*-heterocycles including indole, purine, oxazole, phthalazine, and 1,5-naphthyridine.

functionality **3g** was treated with TMPZnCl·LiCl (2.2 equiv), the two most acidic protons were deprotonated (pK_a(N-H) = 8.3, pK_a(C–H) = 26.9), yielding the zinc reagent **4g** in about 90 % yield.[29] The pK_a values for oxazoles **3h–j** were also calculated.[30] The predictions in oxazole (**3h**, pK_a(H1) = 27.6) and a 4-chlorophenyl substituted oxazole **3i** (pK_a(H1) = 29.9) were correct, with the most acidic site being adjacent to the oxygen atom. However, when these two sites are blocked by substituents as in **3j**, only the least acidic heterocyclic proton remains (pK_a(H1) = 35.4).

Despite the calculated acidity adjacent to the chlorine atom being slightly lower (pK_a(H2) = 35.0), the heterocyclic

C–H bond was deprotonated owing to coordinative effects.[30] Similarly, in phthalazine **3k**[31] and 1,5-naphthyridine **3l**,[7d] electron withdrawing groups (-Cl, -CO*t*Bu) acidify adjacent protons ($pK_a = 31.5–35.8$). Yet, deprotonation occurred at the site of best coordination with the nitrogen atom ($pK_a = 36.3–36.6$, Figure 2).

O- and S-Heterocycles: Inspired by these results, we moved on to investigate oxygen and sulfur heterocycles (7 out of 24 structures are depicted in Figure 3).[20] First, the pK_a values for furan **5a**, which bears both a nitro and an ester functional group, were calculated ($pK_a(H1) = 27.5$, $pK_a(H2) = 25.3$).[22] Similarly to previous cases (**1g**, **3k--m**) the electron withdrawing group leads to a strongly acidified proton in α position. However, deprotonation preferably took place in β-position to the ester group since this carbonyl group is more prone to coordinate the zinc amide base compared to a nitro group. This led to the organozinc **6a** in about 80% yield (25 °C, 0.5 h). Whereas the metalation site of a substituted 2-pyrone **5b**[32] was predicted correctly ($pK_a(H1) = 26.6$, −78 °C, 10 min), the related chromone **5c**[33] led to contrasting results. Here, the coordination to the carbonyl group predominated and deprotonation took place in the thermodynamically less favored site ($pK_a(H1) = 34.0$ versus $pK_a(H2) = 29.8$). Remarkably, this site selectivity could be switched in the related mercapto derivative under optimized reaction conditions. Thus, when **5d** was dissolved in a Et_2O:THF = 1:2 mixture and treated with TMPZnCl·LiCl (−40 °C, 10 min), the reduced polarity led to a selective deprotonation at H2, whereas a non-selective deprotonation occurred in pure THF.[33,34] For other sulfur heterocycles such as benzothiophene **5e**,[22] 1,4-dithiin (**5f**),[35] or 1,4,5,8-tetrathianaphthalene (**5g**),[35] pK_a calculations gave surprisingly low values ($pK_a = 19.9–24.9$). These sites were hence regioselectively deprotonated using the TMP base (−40-25 °C, 0.5 h), to give the corresponding zinc organometallics **6e–g** in circa 90% yield (Figure 3).

Arenes: With the pK_a value of benzene lying at 44.7,[21] deprotonation of unactivated arenes are difficult to achieve and often require harsh reaction conditions.[36] However, when coordinating (-CO_2R, -CO_2NR_2, etc.) or electron withdrawing groups (-NO_2, F, etc.) were present, a metalation could be performed using the mild base TMPZnCl·LiCl (6 out of 23 structures are depicted in Figure 4).[20] Thus, pK_a values for electron-poor arenes **7a–e** were calculated ($pK_a(H1) = 22.6–32.9$) and deprotonation occurred at the most acidic sites at 25–160 °C within 1–7 h, producing the expected arylzinc reagents **8a–e** in 65–80% yield.[22,23,37,38] A reliable prediction for the tropolone scaffold was difficult (**7f**), similarly as with chromone **5c** due to the carbonyl group, which has proven to strongly coordinate to zinc amide bases, inducing a deprotonation in α-position (Figure 4).[39]

Alkenes and Allenes: Next, we investigated the deprotonation of several alkenes and allenes (7 out of 19 structures are depicted in Figure 5).[20] In pK_a calculations following *Approach 1*, geometry optimizations were accompanied by fragmentation and ring-opening reactions.[40] To prevent these structural rearrangements, vertical deprotonation energies (in kJ mol^{-1}) were calculated according to *Approach 2*, where the geometry of the neutral parent was not allowed to relax on deprotonation. With these results in hand, we found that for various alkenes and allenes **9a–f**, the lowest vertical deprotonation energies matched with the actual deprotonation site. Thus, after treatment with TMPZnCl·LiCl (−50–25 °C, 0.25–

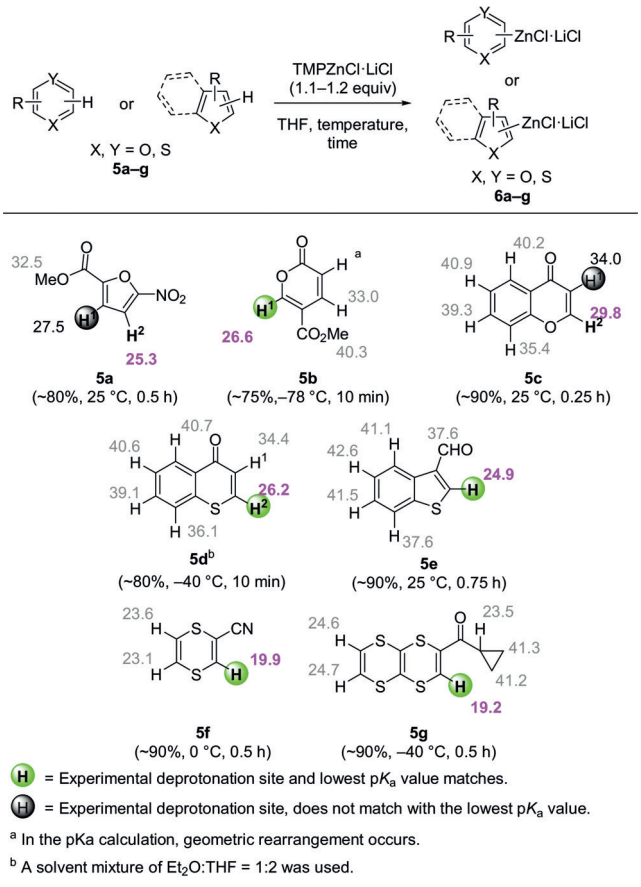

Figure 3. Calculated pK_a values of *O*- and *S*-heterocycles including furane, 2-pyrone, chromone, and benzothiophene.

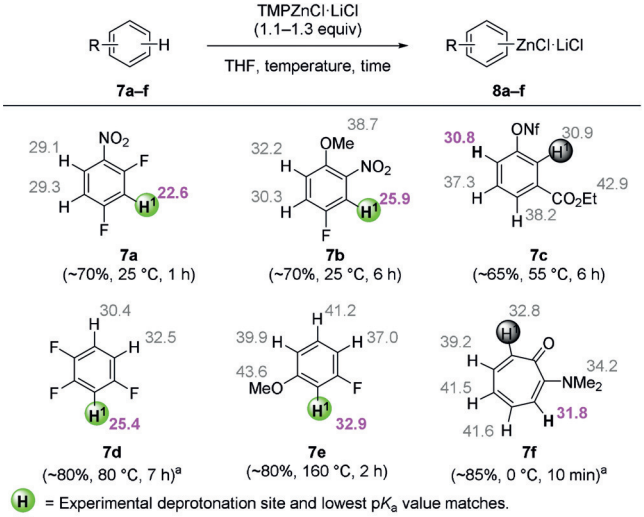

Figure 4. Calculated pK_a values of arenes including a tropolone.

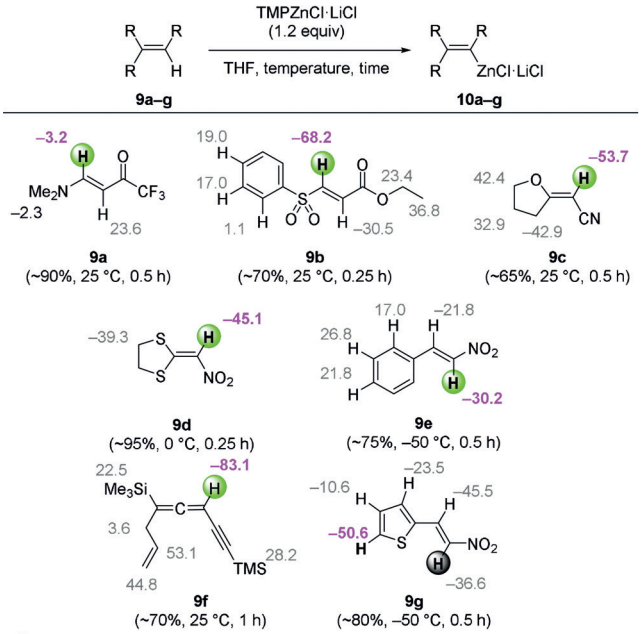

Figure 5. Vertical deprotonation energies [kJ mol^{-1}] calculated according to *Approach 2* for various alkenes and allenes.

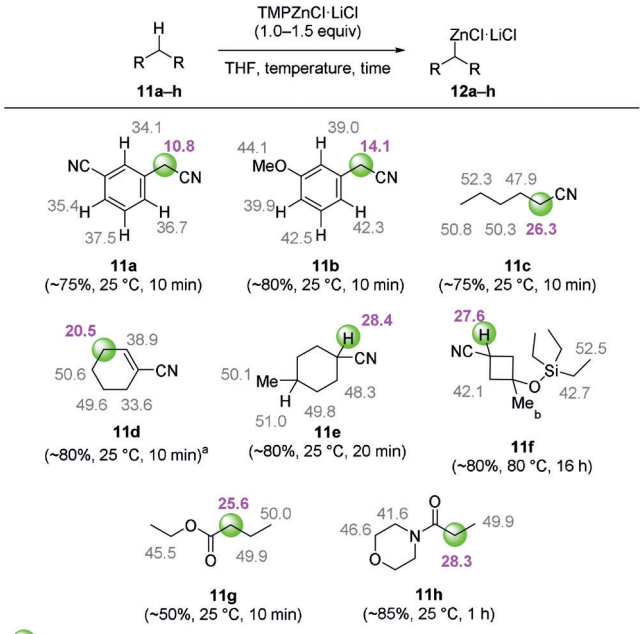

Figure 6. Calculated pK_a values of various functionalized alkanes.

1 h), the zincated alkenes and allenes **10a–f** were obtained in 65–95% yield.[41,42] To ensure that these vertical deprotonation energies are representative for the full study, the respective energies for all other structures were calculated as well (see Supporting Information). Interestingly, the prediction fidelity of *Approach 2* (vertical deprotonation) is closely similar (>80%) as compared to that of *Approach 1* (relaxed deprotonation). In the case of **9g** the lowest energy is given for the proton adjacent to the sulfur atom ($E = -50.6$ kJ mol^{-1}), which seems to bring along a strongly acidifying effect as already observed for other *S*-heterocycles (see **5e–g**). However, also a nitro group, in comparison to the sulfur atom, may coordinate stronger to the zinc amide, which eventually led to a deprotonation adjacent to the nitro group (**9g**, Figure 5).[42]

Alkanes: Finally, various benzylic and alkylic deprotonations were investigated (8 out of 32 structures are depicted in Figure 6).[20] Similarly as in the case of benzene, deprotonations of unactivated alkanes using amide bases occur sluggishly. However, in the presence of stabilizing groups such as nitriles, esters, or amides deprotometalations using TMPZnCl·LiCl may take place.[43] Thus, various benzylic nitriles **11a**,**b**,[44] alkylic nitriles **11c–f**,[8a,44,45] an ester **11g**[44] and an amide (**11h**)[46] were deprotonated at the most acidic position (pK_a = 10.8–28.3), producing alkylzinc organometallics **12a–h** in 50–85% yield (Figure 6).

Novel N-Heterocycles: To demonstrate the utility of the developed predictive model, several so far unexplored *N*-heterocycles were investigated towards metalations using TMPZnCl·LiCl. After having calculated the pK_a values (see Figure 7), all six *N*-heterocycles **13a–e** were treated with TMPZnCl·LiCl (1.2 equiv) and quenched with various electrophiles (Scheme 2). The deprotonation sites were confirmed by deuteration of the reaction mixtures followed by ^{1}H NMR analysis (see Supporting Information). Thus, pyrido[2,3-*b*]pyrazine (**13a**), imidazo[1,2-*b*]pyridazine (**13b**), [1,2,4]triazolo[4,3-*a*]pyrazine (**13c**), and [1,2,4]triazolo[1,5-*a*]pyrimidine (**13d**) were readily deprotonated in the predicted most acidic positions (pK_a = 24.6–34.6), leading to organozinc reagents **14a–d** in 40–70% yield. After iodolysis or

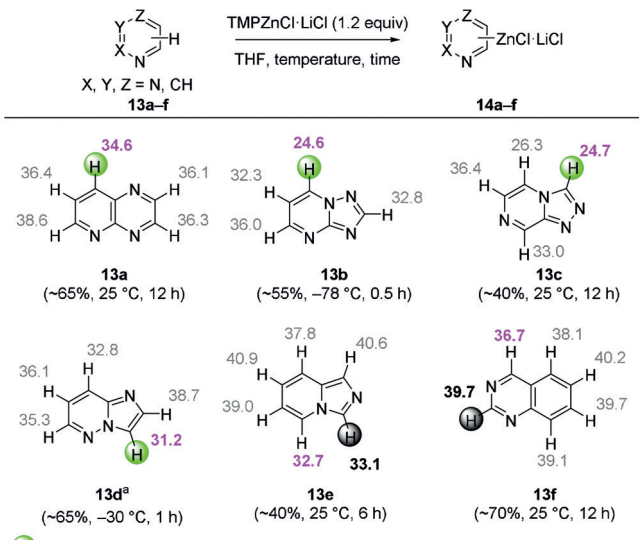

Figure 7. Calculated pK_a values of non-investigated *N*-heterocycles.

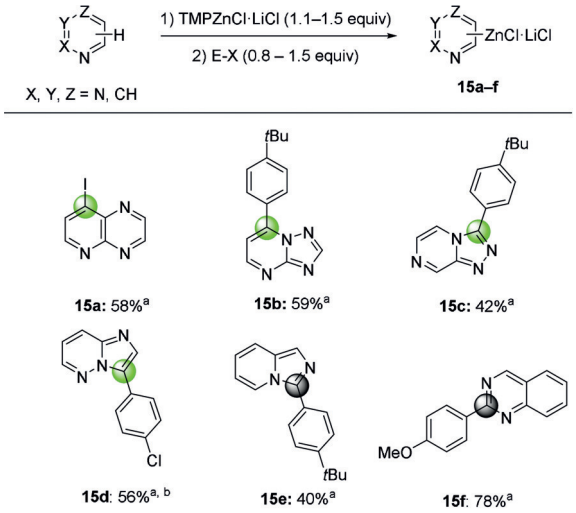

a Isolated yield.
b $TMP_2Zn{\cdot}2MgCl_2{\cdot}2LiCl$ (1.2 equiv) was used

Scheme 2. Deprotonation and functionalization of various non-investigated *N*-heterocycles using TMPZnCl·LiCl.

palladium-catalyzed Negishi cross-couplings[47] the expected *N*-heterocycles **15a–d** were obtained in 42–59% yield (Scheme 2). It is noteworthy, that in the case of **13d**, the stronger base $TMP_2Zn{\cdot}2\,MgCl_2{\cdot}2\,LiCl$ was used to achieve zincation, since TMPZnCl·LiCl reacted sluggishly. In imidazo[1,5-*a*]pyridine (**13e**), two protons have similar pK_a values (pK_a(H1) = 33.1, pK_a(H2) = 32.7). Since coordination to a nitrogen atom can only take place at position C1, TMPZnCl·LiCl preferably deprotonates proton H1, leading, after cross-coupling, to the functionalized *N*-heterocycle **15e** in 40% yield. The pK_a values in quinazoline (**13f**) are relatively high (pK_a = 36.7–40.2), resulting in a deprotonation only at the site of best coordination, which lies in between the two nitrogen atoms (C2). After electrophilic quenching, the biaryl **15f** was obtained in 78% yield.

Evaluating the success of the theoretical approaches employed herein, we found that the pK_a values calculated according to *Approach 1* predict the correct deprotonation site as the site of highest acidity in 81.4% of all cases (Figure 8). The use of vertical deprotonation energies (VDEs) led to improved predictions not only for the alkene substrates, where anion formation triggered larger structural rearrangements untypical for the actual metalated species, but also for the complete dataset study with a prediction fidelity of 82.5%. This result may imply that the unrelaxed anions obtained through vertical deprotonation of the neutral parents are structurally more similar to a metalated species than the structurally relaxed anions obtained after geometry optimization. A final remark should be made for substrates, where the pK_a values differed by less than one unit (such as **13e** in Figure 7). If these cases are counted as successful predictions, the fidelity of the prediction increased to more than 88% (Figure 8C, the prediction is considered successful if the VDE associated with experimentally determined site lies within 5.69 kJ mol^{-1} (1 pK_a unit) window to the lowest VDE value in the molecule).

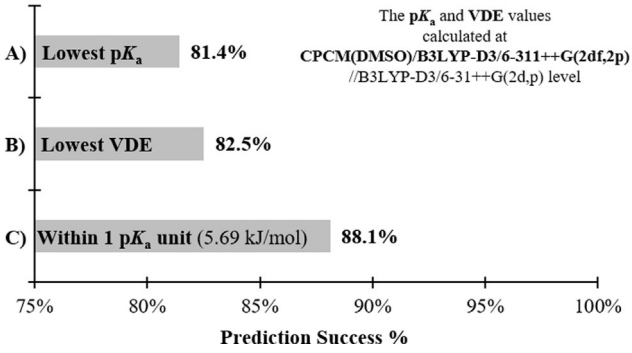

Figure 8. Prediction success rates for the experimentally determined site of metalation using the pK_a values and vertical deprotonation energies (VDEs) for the molecules depicted in Figures 1–6 (see Figure S7 in the Supporting Information for details).

Conclusion

In summary, we have developed a model which allowed site-selective predictions in deprotometalation reactions of various organic molecules bearing relatively acidic protons using TMPZnCl·LiCl. A wide range of *N*-, *S*-, and *O*-heterocycles as well as functionalized arenes, alkenes and alkanes were investigated and their pK_a values calculated. Overall, the predicted site matched well with the empirical results, with a correct prediction in over 80% of the more than 150 investigated substrates, suggesting that for the relatively covalent zinc amide TMPZnCl·LiCl, thermodynamic considerations predominate. It may also be anticipated that in the case of stronger bases, kinetic effects such as the CIPE are of greater importance, which would lead to a more difficult prediction. Finally, the model was used to help predicting the deprotonation site of six so far non-disclosed *N*-heterocycles.

Acknowledgements

We thank the DFG for financial support. We also thank Albemarle (Hoechst, Germany) and BASF (Ludwigshafen, Germany) for the generous gift of chemicals. We would also like to thank the Leibniz Supercomputing Centre (http://www.lrz.de) for generous allocation of computational resources.

Conflict of interest

The authors declare no conflict of interest.

Keywords: acidity · amides · heteroarenes · predictive models · zinc organometallics

[1] a) W. R. Pitt, D. M. Parry, B. G. Perry, C. R. Groom, *J. Med. Chem.* **2009**, *52*, 2952–2963; b) R. D. Taylor, M. MacCoss, A. D. G. Lawson, *J. Med. Chem.* **2014**, *57*, 5845–5859; c) E. Vitaku, D. T. Smith, J. T. Njardarson, *J. Med. Chem.* **2014**, *57*, 10257–10274; d) P. Martins, J. Jesus, S. Santos, L. R. Raposo, C. Roma-Rodrigues, P. V. Baptista, A. R. Fernandes,*Molecules*

2015, *20*, 16852; e) K. Dinesh, J. Subheet Kumar, *Curr. Med. Chem.* **2016**, *23*, 4338 – 4394; f) A. P. Taylor, R. P. Robinson, Y. M. Fobian, D. C. Blakemore, L. H. Jones, O. Fadeyi, *Org. Biomol. Chem.* **2016**, *14*, 6611 – 6637; g) M. D. Polêto, V. H. Rusu, B. I. Grisci, M. Dorn, R. D. Lins, H. Verli, *Front. Pharmacol.* **2018**, *9*, 1 – 20.

[2] A. Mullard, *Nat. Rev. Drug Discovery* **2019**, *18*, 85 – 89.

[3] a) T. W. Lyons, M. S. Sanford, *Chem. Rev.* **2010**, *110*, 1147 – 1169; b) T. Gensch, M. N. Hopkinson, F. Glorius, J. Wencel-Delord, *Chem. Soc. Rev.* **2016**, *45*, 2900 – 2936; c) K. Murakami, S. Yamada, T. Kaneda, K. Itami, *Chem. Rev.* **2017**, *117*, 9302 – 9332; d) H. M. L. Davies, D. Morton, *ACS Cent. Sci.* **2017**, *3*, 936 – 943; e) Z. Dong, Z. Ren, S. J. Thompson, Y. Xu, G. Dong, *Chem. Rev.* **2017**, *117*, 9333 – 9403; f) Y. Wei, P. Hu, M. Zhang, W. Su, *Chem. Rev.* **2017**, *117*, 8864 – 8907; g) Y. Yang, J. Lan, J. You, *Chem. Rev.* **2017**, *117*, 8787 – 8863; h) R. H. Crabtree, A. Lei, *Chem. Rev.* **2017**, *117*, 8481 – 8482; i) J. C. K. Chu, T. Rovis, *Angew. Chem. Int. Ed.* **2018**, *57*, 62 – 101; *Angew. Chem.* **2018**, *130*, 64 – 105; j) P. Gandeepan, L. Ackermann, *Chem* **2018**, *4*, 199 – 222; k) P. Gandeepan, T. Müller, D. Zell, G. Cera, S. Warratz, L. Ackermann, *Chem. Rev.* **2019**, *119*, 2192 – 2452.

[4] a) V. Snieckus, *Chem. Rev.* **1990**, *90*, 879 – 933; b) F. Mongin, G. Quéguiner, *Tetrahedron* **2001**, *57*, 4059 – 4090; c) A. Turck, N. Plé, F. Mongin, G. Quéguiner, *Tetrahedron* **2001**, *57*, 4489 – 4505; d) R. E. Mulvey, *Organometallics* **2006**, *25*, 1060 – 1075; e) R. E. Mulvey, F. Mongin, M. Uchiyama, Y. Kondo, *Angew. Chem. Int. Ed.* **2007**, *46*, 3802 – 3824; *Angew. Chem.* **2007**, *119*, 3876 – 3899; f) R. E. Mulvey, *Acc. Chem. Res.* **2009**, *42*, 743 – 755; g) B. Haag, M. Mosrin, H. Ila, V. Malakhov, P. Knochel, *Angew. Chem. Int. Ed.* **2011**, *50*, 9794 – 9824; *Angew. Chem.* **2011**, *123*, 9968 – 9999; h) D. Tilly, F. Chevallier, F. Mongin, P. C. Gros, *Chem. Rev.* **2014**, *114*, 1207 – 1257; i) F. Mongin, A. Harrison-Marchand, *Chem. Rev.* **2013**, *113*, 7563 – 7727; j) P. J. Harford, A. J. Peel, F. Chevallier, R. Takita, F. Mongin, M. Uchiyama, A. E. H. Wheatley, *Dalton Trans.* **2014**, *43*, 14181 – 14203; k) T. Klatt, J. T. Markiewicz, C. Sämann, P. Knochel, *J. Org. Chem.* **2014**, *79*, 4253 – 4269; l) F. Chevallier, F. Mongin, R. Takita, M. Uchiyama, *Arene Chemistry*, Wiley, Hoboken, **2015**, pp. 777 – 812; m) J. García-Álvarez, E. Hevia, V. Capriati, *Eur. J. Org. Chem.* **2015**, 6779 – 6799; n) *Handbook of Reagents for Organic Synthesis: Reagents for Heteroarene Functionalization* (Eds.: A. B. Charette), Wiley-VCH, Weinheim, **2015**; o) M. Uzelac, A. R. Kennedy, E. Hevia, *Inorg. Chem.* **2017**, *56*, 8615 – 8626; p) M. Balkenhohl, P. Knochel, *SynOpen* **2018**, *02*, 78 – 95; q) S. D. Robertson, M. Uzelac, R. E. Mulvey, *Chem. Rev.* **2019**, *119*, 8332 – 8405.

[5] a) T. Imahori, M. Uchiyama, T. Sakamoto, Y. Kondo, *Chem. Commun.* **2001**, 2450 – 2451; b) M. Schlosser, *Angew. Chem. Int. Ed.* **2005**, *44*, 376 – 393; *Angew. Chem.* **2005**, *117*, 380 – 398; c) M. Alessi, A. L. Larkin, K. A. Ogilvie, L. A. Green, S. Lai, S. Lopez, V. Snieckus, *J. Org. Chem.* **2007**, *72*, 1588 – 1594; d) S. K. Verma, L. V. LaFrance, *Tetrahedron Lett.* **2009**, *50*, 383 – 385; e) C. Schneider, E. Broda, V. Snieckus, *Org. Lett.* **2011**, *13*, 3588 – 3591; f) Z. Zhang, L. P. Dwoskin, P. A. Crooks, *Tetrahedron Lett.* **2011**, *52*, 2667 – 2669; g) F. Crestey, G. Hooyberghs, J. L. Kristensen, *Tetrahedron* **2012**, *68*, 1417 – 1421; h) C. S. Demmer, M. Jørgensen, J. Kehler, L. Bunch, L. K. Rasmussen, *Synlett* **2015**, *26*, 519 – 524; i) A. I. Subota, O. O. Grygorenko, Y. B. Valter, M. A. Tairov, O. S. Artamonov, D. M. Volochnyuk, S. V. Ryabukhin, *Synlett* **2015**, *26*, 408 – 411.

[6] a) A. Turck, N. Plé, L. Mojovic, G. Quéguiner, *J. Heterocycl. Chem.* **1990**, *27*, 1377 – 1381; b) J. E. torr, J. M. Large, P. N. Horton, M. B. Hursthouse, E. McDonald, *Tetrahedron Lett.* **2006**, *47*, 31 – 34; c) M. Uzelac, A. R. Kennedy, E. Hevia, R. E. Mulvey, *Angew. Chem. Int. Ed.* **2016**, *55*, 13147 – 13150; *Angew. Chem.* **2016**, *128*, 13341 – 13344.

[7] For recent examples, see: a) B. Melzer, A. Plodek, F. Bracher, *J. Org. Chem.* **2014**, *79*, 7239 – 7242; b) M. F. Z. J. Amaral, A. A. Baumgartner, R. Vessecchi, G. C. Clososki, *Org. Lett.* **2015**, *17*, 238 – 241; c) A. Plodek, M. König, F. Bracher, *Eur. J. Org. Chem.* **2015**, 1302 – 1308; d) M. Balkenhohl, R. Greiner, I. S. Makarov, B. Heinz, K. Karaghiosoff, H. Zipse, P. Knochel, *Chem. Eur. J.* **2017**, *23*, 13046 – 13050; e) M. Balkenhohl, C. François, D. Sustac Roman, P. Quinio, P. Knochel, *Org. Lett.* **2017**, *19*, 536 – 539; f) C. R. d. S. Bertallo, T. R. Arroio, M. F. Z. J. Toledo, S. A. Sadler, R. Vessecchi, P. G. Steel, G. C. Clososki, *Eur. J. Org. Chem.* **2019**, 5205 – 5213; g) B. C. Melzer, A. Plodek, F. Bracher, *Beilstein J. Org. Chem.* **2019**, *15*, 2304 – 2310.

[8] For recent examples, see: a) M. E. Dalziel, P. Chen, D. E. Carrera, H. Zhang, F. Gosselin, *Org. Lett.* **2017**, *19*, 3446 – 3449; b) L. Klier, D. S. Ziegler, R. Rahimoff, M. Mosrin, P. Knochel, *Org. Process Res. Dev.* **2017**, *21*, 660 – 663; c) M. Balkenhohl, H. Jangra, T. Lenz, M. Ebeling, H. Zipse, K. Karaghiosoff, P. Knochel, *Angew. Chem. Int. Ed.* **2019**, *58*, 9244 – 9247; *Angew. Chem.* **2019**, *131*, 9344 – 9348.

[9] a) A. Seggio, F. Chevallier, M. Vaultier, F. Mongin, *J. Org. Chem.* **2007**, *72*, 6602 – 6605; b) F. Chevallier, F. Mongin, *Chem. Soc. Rev.* **2008**, *37*, 595 – 609; c) M. Mosrin, P. Knochel, *Org. Lett.* **2008**, *10*, 2497 – 2500; d) M. Mosrin, P. Knochel, *Chem. Eur. J.* **2009**, *15*, 1468 – 1477; e) M. Mosrin, T. Bresser, P. Knochel, *Org. Lett.* **2009**, *11*, 3406 – 3409; f) A. Unsinn, M. J. Ford, P. Knochel, *Org. Lett.* **2013**, *15*, 1128 – 1131.

[10] a) F. Chevallier, Y. S. Halauko, C. Pecceu, I. F. Nassar, T. U. Dam, T. Roisnel, V. E. Matulis, O. A. Ivashkevich, F. Mongin, *Org. Biomol. Chem.* **2011**, *9*, 4671 – 4684; b) K. Snégaroff, T. T. Nguyen, N. Marquise, Y. S. Halauko, P. J. Harford, T. Roisnel, V. E. Matulis, O. A. Ivashkevich, F. Chevallier, A. E. H. Wheatley, P. C. Gros, F. Mongin, *Chem. Eur. J.* **2011**, *17*, 13284 – 13297; c) R. R. Kadiyala, D. Tilly, E. Nagaradja, T. Roisnel, V. E. Matulis, O. A. Ivashkevich, Y. S. Halauko, F. Chevallier, P. C. Gros, F. Mongin, *Chem. Eur. J.* **2013**, *19*, 7944 – 7960; d) N. Marquise, G. Bretel, F. Lassagne, F. Chevallier, T. Roisnel, V. Dorcet, Y. S. Halauko, O. A. Ivashkevich, V. E. Matulis, P. C. Gros, F. Mongin, *RSC Adv.* **2014**, *4*, 19602 – 19612; e) M. Y. A. Messaoud, G. Bentabed-Ababsa, M. Hedidi, A. Derdour, F. Chevallier, Y. S. Halauko, O. A. Ivashkevich, V. E. Matulis, L. Picot, V. Thiéry, T. Roisnel, V. Dorcet, F. Mongin, *Beilstein J. Org. Chem.* **2015**, *11*, 1475 – 1485; f) E. Nagaradja, G. Bentabed-Ababsa, M. Scalabrini, F. Chevallier, S. Philippot, S. Fontanay, R. E. Duval, Y. S. Halauko, O. A. Ivashkevich, V. E. Matulis, T. Roisnel, F. Mongin, *Bioorg. Med. Chem.* **2015**, *23*, 6355 – 6363; g) M. Hedidi, G. Bentabed-Ababsa, A. Derdour, Y. S. Halauko, O. A. Ivashkevich, V. E. Matulis, F. Chevallier, T. Roisnel, V. Dorcet, F. Mongin, *Tetrahedron* **2016**, *72*, 2196 – 2205; h) M. Hedidi, J. Maillard, W. Erb, F. Lassagne, Y. S. Halauko, O. A. Ivashkevich, V. E. Matulis, T. Roisnel, V. Dorcet, M. Hamzé, Z. Fajloun, B. Baratte, S. Ruchaud, S. Bach, G. Bentabed-Ababsa, F. Mongin, *Eur. J. Org. Chem.* **2017**, 5903 – 5915; For an accurate prediction of pK_a values using graph convolutional neural networks, see: i) R. Roszak, W. Beker, K. Molga, B. A. Grzybowski, *J. Am. Chem. Soc.* **2019**, *141*, 17142 – 17149.

[11] a) M. C. Whisler, S. MacNeil, V. Snieckus, P. Beak, *Angew. Chem. Int. Ed.* **2004**, *43*, 2206 – 2225; *Angew. Chem.* **2004**, *116*, 2256 – 2276; Also, exceptional metalation selectivities were observed when well defined template bases were used in deprotometalation reactions, see: b) A. J. Martínez-Martínez, A. R. Kennedy, R. E. Mulvey, C. T. O'Hara, *Science* **2014**, *346*, 834 – 837; c) A. J. Martínez-Martínez, D. R. Armstrong, B. Conway, B. J. Fleming, J. Klett, A. R. Kennedy, R. E. Mulvey, S. D. Robertson, C. T. O'Hara, *Chem. Sci.* **2014**, *5*, 771 – 781; d) A. J. Martínez-Martínez, S. Justice, B. J. Fleming, A. R. Kennedy, I. D. H. Oswald, C. T. O'Hara, *Sci. Adv.* **2017**, *3*, e1700832.

[12] L. Pauling, *The Nature of the Chemical Bond-An Introduction to Modern Structural Chemistry*, 3rd ed., Cornell University Press, Ithaca, **1960**.
[13] a) P. Gros, S. Choppin, Y. Fort, *J. Org. Chem.* **2003**, *68*, 2243 – 2247; b) A. Frischmuth, M. Fernández, N. M. Barl, F. Achrainer, H. Zipse, G. Berionni, H. Mayr, K. Karaghiosoff, P. Knochel, *Angew. Chem. Int. Ed.* **2014**, *53*, 7928 – 7932; *Angew. Chem.* **2014**, *126*, 8062 – 8066.
[14] For theoretical models and their application in synthetic organic chemistry, see: a) P. E. Gormisky, M. C. White, *J. Am. Chem. Soc.* **2013**, *135*, 14052 – 14055; b) F. O'Hara, D. G. Blackmond, P. S. Baran, *J. Am. Chem. Soc.* **2013**, *135*, 12122 – 12134; c) E. N. Bess, D. M. Guptill, H. M. L. Davies, M. S. Sigman, *Chem. Sci.* **2015**, *6*, 3057 – 3062; d) K. A. Margrey, J. B. McManus, S. Bonazzi, F. Zecri, D. A. Nicewicz, *J. Am. Chem. Soc.* **2017**, *139*, 11288 – 11299.
[15] A. D. Becke, *J. Chem. Phys.* **1993**, *98*, 5648 – 5652.
[16] a) S. Grimme, J. Antony, S. Ehrlich, H. Krieg, *J. Chem. Phys.* **2010**, *132*, 154104; b) S. Grimme, *J. Comput. Chem.* **2006**, *27*, 1787 – 1799.
[17] a) R. Ditchfield, W. J. Hehre, J. A. Pople, *J. Chem. Phys.* **1971**, *54*, 724 – 728; b) R. Krishnan, J. S. Binkley, R. Seeger, J. A. Pople, *J. Chem. Phys.* **1980**, *72*, 650 – 654.
[18] M. Cossi, N. Rega, G. Scalmani, V. Barone, *J. Comput. Chem.* **2003**, *24*, 669 – 681.
[19] Yields of organometallic arylzinc reagents are estimated to be 5% higher than the products obtained after electrophilic trapping reactions and were rounded to the nearest 5%.
[20] For complete calculation data and additional structures, see the Supporting Information.
[21] a) K. Shen, Y. Fu, J.-N. Li, L. Liu, Q.-X. Guo, *Tetrahedron* **2007**, *63*, 1568 – 1576; b) When pyridine was treated with TMPZnCl·LiCl in THF, no metalation took place.
[22] M. Mosrin, P. Knochel, *Org. Lett.* **2009**, *11*, 1837 – 1840.
[23] T. Bresser, M. Mosrin, G. Monzon, P. Knochel, *J. Org. Chem.* **2010**, *75*, 4686 – 4695.
[24] M. Mosrin, G. Monzon, T. Bresser, P. Knochel, *Chem. Commun.* **2009**, 5615 – 5617.
[25] F. Gosselin, S. J. Savage, N. Blaquiere, S. T. Staben, *Org. Lett.* **2012**, *14*, 862 – 865.
[26] M. Balkenhohl, B. Salgues, T. Hirai, K. Karaghiosoff, P. Knochel, *Org. Lett.* **2018**, *20*, 3114 – 3118.
[27] B. V. Lam, Y. Berhault, S. Stiebing, C. Fossey, T. Cailly, V. Collot, F. Fabis, *Chem. Eur. J.* **2016**, *22*, 4440 – 4446.
[28] F. Crestey, S. Zimdars, P. Knochel, *Synthesis* **2013**, *45*, 3029 – 3037.
[29] J. Shen, B. Wong, C. Gu, H. Zhang, *Org. Lett.* **2015**, *17*, 4678 – 4681.
[30] D. Haas, M. Mosrin, P. Knochel, *Org. Lett.* **2013**, *15*, 6162 – 6165.
[31] F. Crestey, P. Knochel, *Synthesis* **2010**, 1097 – 1106.
[32] D. S. Ziegler, L. Klier, N. Müller, K. Karaghiosoff, P. Knochel, *Synthesis* **2018**, *50*, 4383 – 4394.
[33] L. Klier, T. Bresser, T. A. Nigst, K. Karaghiosoff, P. Knochel, *J. Am. Chem. Soc.* **2012**, *134*, 13584 – 13587.
[34] Due to reduction of the polarity, a stronger coordination of TMPZnCl·LiCl to the sulfur atom took place.
[35] A. Castelló-Micó, J. Nafe, K. Higashida, K. Karaghiosoff, M. Gingras, P. Knochel, *Org. Lett.* **2017**, *19*, 360 – 363.
[36] A. B. Bellan, P. Knochel, *Angew. Chem. Int. Ed.* **2019**, *58*, 1838 – 1841; *Angew. Chem.* **2019**, *131*, 1852 – 1856.
[37] G. Monzon, P. Knochel, *Synlett* **2010**, 304 – 308.
[38] S. Otsuka, H. Yorimitsu, A. Osuka, *Chem. Eur. J.* **2015**, *21*, 14703 – 14707.
[39] D. Haas, D. Sustac-Roman, S. Schwarz, P. Knochel, *Org. Lett.* **2016**, *18*, 6380 – 6383.
[40] See the Supporting Information for further details.
[41] T. Bresser, P. Knochel, *Angew. Chem. Int. Ed.* **2011**, *50*, 1914 – 1917; *Angew. Chem.* **2011**, *123*, 1954 – 1958.
[42] P. Quinio, C. François, A. Escribano Cuesta, A. K. Steib, F. Achrainer, H. Zipse, K. Karaghiosoff, P. Knochel, *Org. Lett.* **2015**, *17*, 1010 – 1013.
[43] For magnesiations and lithiations of alkylnitriles, see: a) F. F. Fleming, S. Gudipati, Z. Zhang, W. Liu, O. W. Steward, *J. Org. Chem.* **2005**, *70*, 3845 – 3849; b) F. F. Fleming, W. Liu, S. Ghosh, O. W. Steward, *J. Org. Chem.* **2008**, *73*, 2803 – 2810; c) F. F. Fleming, S. Gudipati, *Eur. J. Org. Chem.* **2008**, 5365 – 5374; d) G. Barker, M. R. Alshawish, M. C. Skilbeck, I. Coldham, *Angew. Chem. Int. Ed.* **2013**, *52*, 7700 – 7703; *Angew. Chem.* **2013**, *125*, 7854 – 7857; e) A. Sadhukhan, M. C. Hobbs, A. J. H. M. Meijer, I. Coldham, *Chem. Sci.* **2017**, *8*, 1436 – 1441.
[44] S. Duez, S. Bernhardt, J. Heppekausen, F. F. Fleming, P. Knochel, *Org. Lett.* **2011**, *13*, 1690 – 1693.
[45] R. J. Mycka, S. Duez, S. Bernhardt, J. Heppekausen, P. Knochel, F. F. Fleming, *J. Org. Chem.* **2012**, *77*, 7671 – 7676.
[46] Y. H. Chen, M. Ellwart, G. Toupalas, Y. Ebe, P. Knochel, *Angew. Chem. Int. Ed.* **2017**, *56*, 4612 – 4616; *Angew. Chem.* **2017**, *129*, 4683 – 4687.
[47] a) A. O. King, N. Okukado, E.-i. Negishi, *J. Chem. Soc. Chem. Commun.* **1977**, 683; b) D. Haas, J. M. Hammann, R. Greiner, P. Knochel, *ACS Catal.* **2016**, *6*, 1540 – 1552.

Manuscript received: April 13, 2020
Accepted manuscript online: May 12, 2020
Version of record online: June 8, 2020

